Affinity for the nuclear compartment and expression during cell differentiation implicate phosphorylated Groucho/TLE1 forms of higher molecular mass in nuclear functions

Junaid HUSAIN, Rita LO, Diane GRBAVEC and Stefano STIFANI*

Center for Neuronal Survival, Montreal Neurological Institute, McGill University, 3801 rue University, Montreal, Quebec, H3A 2B4 Canada

The *Drosophila* protein Groucho is involved in embryonic segmentation and neural development, and is implicated in the Notch signal transduction pathway. We are investigating the molecular mechanisms underlying the function of Groucho and of its mammalian homologues, the TLE ('**t**ransducin-**l**ike **E**nhancer of split') proteins. We show that Groucho/TLE1 proteins are phosphorylated. We also show that two populations of phosphorylated Groucho proteins can be identified based on their interaction with the nuclear compartment. More slowly migrating proteins with an apparent molecular mass of roughly 110 kDa interact strongly with the nuclei, while faster migrating proteins displaying molecular masses of roughly 84–85 kDa show lower affinity for the nuclear compartment. Similarly, TLE1 proteins with an apparent molecular mass of roughly 118 kDa exhibit higher affinity for the nuclear compartment than do faster migrating forms with apparent molecular masses of 90–93 kDa. Moreover, we show that the nuclear, more slowly migrating, TLE1 proteins are induced during neural determination of P19 embryonic carcinoma cells. These results implicate phosphorylation in the activity of Groucho/TLE1 proteins and suggest that phosphorylated forms of higher molecular mass are involved in nuclear functions. Finally, we show that different TLE proteins respond in different ways to the neural commitment of P19 cells, suggesting that individual members of this protein family may have non-redundant functions.

INTRODUCTION

The Notch signal transduction pathway is an evolutionarily conserved mechanism controlling the specification of a variety of fates, including neural, epithelial, muscle and haematopoietic lineages (reviewed in [1,2]). The molecular mechanisms underlying Notch signalling are not well understood. The products of a number of genes that exhibit phenotypic interactions with *Notch* were implicated in the Notch cascade in *Drosophila* [2]. Some of these proteins were shown to interact directly with the Notch receptor [3–5], while others are thought to indirectly mediate downstream responses following interaction of Notch with extracellular ligands [2]. Among these latter molecules, two groups of proteins appear to be important intracellular mediators of Notch signalling. These are the products of the *groucho* gene [6,7] and of the *hairy/Enhancer of split* complex [8–11] gene family. While *hairy* and the *Enhancer of split* complex encode closely related DNA-binding proteins containing the basic helix–loop–helix motif [8–11], *groucho* encodes a protein resembling yeast Tup1 [12], a protein involved in the regulation of gene expression [13]. The characterization of Groucho homologues, designated the TLE ('**t**ransducin-**l**ike **E**nhancer of split') proteins, from humans [14] and rodents [15–17] showed that Groucho/TLE proteins share a number of conserved structural motifs that are implicated in nuclear functions. These features are in agreement with the observations that both Groucho [18] and TLE [14,19–21] proteins are detected in the nuclei and that Groucho interacts with the basic helix–loop–helix DNA-binding proteins of the Hairy/Enhancer of split family [22]. These interactions are believed to lead to the formation of transcription complexes that mediate at least some of the functions of the Notch pathway by negatively regulating the expression and/or function of target differentiation genes [22–24].

We are interested in understanding the mechanisms that regulate the nuclear functions of Groucho/TLE proteins and how these mechanisms may respond to changes in the physiological environment. We show here that Groucho/TLE proteins are phosphorylated and that two populations of phosphorylated Groucho proteins can be identified based on their interaction with the nuclear compartment. More slowly migrating proteins with an apparent molecular mass of roughly 110 kDa are strongly associated with the nuclei, while faster migrating proteins displaying molecular masses of roughly 84–85 kDa show reduced affinity for the nuclear compartment. Phosphorylated TLE1 proteins display similar behaviours: larger forms with an apparent molecular mass of roughly 118 kDa exhibit higher affinity for the nuclear compartment than faster migrating forms with apparent molecular masses of 90–93 kDa. We also show that the nuclear, more slowly migrating, TLE1 proteins are induced during neural determination of P19 embryonic carcinoma cells. These results implicate phosphorylation in the activity of Groucho/TLE1 proteins and suggest that phosphorylated forms of higher molecular mass are involved in nuclear functions. Finally, we show that different TLE proteins respond in different ways to the neural commitment of P19 cells and are differentially expressed in T lymphoblastic leukaemia cells, suggesting that individual members of this protein family may have non-redundant functions.

MATERIALS AND METHODS

Cell culture, preparation of cell and tissue lysates, and Northern blotting

Drosophila S2 cells [25], and human HeLa [14], Jurkat [26], CCRF-CEM [27] and SUP-T1 [28] cells were cultured as de-

Abbreviation used: GST, glutathione S-transferase; TLE, **t**ransducin-**l**ike **E**nhancer of split.

* To whom correspondence should be addressed.

scribed previously. Mouse P19 embryonic carcinoma cells were cultured and induced to undergo neural determination as described in [29]. Briefly, exponentially growing P19 cells were plated (10^5 cells/ml) in culture medium [minimal essential medium supplemented with 10% (v/v) fetal bovine serum] containing 0.3 μM retinoic acid. Cells cultured prior to the addition of retinoic acid are defined as 'day 0' cells. After 2 days, cells were transferred to bacterial-grade Petri dishes, where they were allowed to aggregate for 1 day. On the following day, cell aggregates were plated on to tissue-culture-grade dishes, and the culture medium was replaced every 2 days. Induction was normally terminated 10 days after addition of retinoic acid ('day 10'). For the preparation of whole-cell lysates, cultured cells were homogenized in ice-cold buffer A [30 mM Hepes (pH 7.6), 60 mM KCl, 30 mM NaCl, 1 mM EDTA, 200 mM sucrose, 20 mM iodoacetamide, 1 mM PMSF, 2 μM leupeptin, 2.5 μg/ml aprotinin, 2.5 μg/ml pepstatin A and 2.5 μg/ml antipain] by trituration through 25-gg needles, and lysed in the presence of 1% Triton X-100. Lysates were centrifuged at 12000 ***g*** for 15 min and the supernatant was recovered and used for subsequent analysis. Northern blotting with a *TLE1*-specific probe was as described in [14].

Preparation of subcellular fractions

Post-nuclear supernatant and nuclear fractions were prepared as described in [30]. Briefly, cells were washed twice with either PBS (P19 cells) or balanced salt solution (S2 cells), harvested, and resuspended for 10 s in ice-cold hypotonic buffer [20 mM Hepes (pH 7.6), 10 mM KCl, 1.5 mM $MgCl_2$, 0.5 mM dithiothreitol, 1 mM PMSF, 2 μM leupeptin, 2.5 μg/ml aprotinin, 2.5 μg/ml pepstatin A and 2.5 μg/ml antipain]. Cells were collected by centrifugation, resuspended in 5–8 packed cell pellet volumes of hypotonic buffer and allowed to stand on ice for 10 min, after which the cell suspension was triturated through a 25-gg needle. The homogenate then received 0.5 cell pellet volumes of buffer B [50 mM Hepes (pH 7.6), 1 M KCl, 30 mM $MgCl_2$, 0.5 mM EDTA, 1 mM PMSF, 2 μM leupeptin, 2.5 μg/ml aprotinin, 2.5 μg/ml pepstatin A and 2.5 μg/ml antipain] and was mixed thoroughly, followed by centrifugation at 300 ***g*** for 1 min to remove cell debris. The supernatant was centrifuged at 1500 ***g*** for 15 min and the resulting supernatant was collected (post-nuclear supernatant). The crude nuclear pellet was washed twice with 10–20 packed cell pellet volumes of hypotonic buffer, and the nuclei were collected by centrifugation at 1500 ***g*** for 15 min and resuspended in 2 volumes of buffer C [20 mM Hepes (pH 7.6), 500 mM NaCl, 0.5 mM EDTA, 1% Triton X-100, 1 mM PMSF, 2 μM leupeptin, 2.5 μg/ml aprotinin, 2.5 μg/ml pepstatin A and 2.5 μg/ml antipain]. Post-nuclear supernatants and nuclear fractions were mixed with equal volumes of 2× electrophoresis sample buffer [125 mM Tris/HCl (pH 6.8), 20% glycerol, 4% SDS and 100 mM dithiothreitol], passed through a 25-gg needle, heated to 95 °C for 5 min and subjected to SDS/PAGE. SDS/PAGE, transfer to nitrocellulose and Western blotting in the presence of the Groucho monoclonal supernatant 3C (diluted 1:20) [18], the panTLE monoclonal supernatant (1:20) [14] or TLE polyclonal antibodies (1:1000) were as described previously [14]. Bound antibodies were visualized by incubation with horseradish peroxidase-conjugated secondary antibodies (1:4000), followed by enhanced chemiluminescence detection.

Phosphorylation and immunoprecipitation of Groucho and TLE1, and phosphoamino acid analysis

In a typical metabolic labelling reaction with [^{32}P]P_i, 10–15 ml of S2 cell suspension (approx. 2×10^7 cells/ml) was used. Cells were collected, washed twice with balanced salt solution, resuspended in phosphate-free M3 medium and incubated at 24 °C for 45 min. Then cells were incubated for 3 h in the presence of 750 μCi/ml [^{32}P]P_i (Amersham; 370 MBq/ml). At the end of this incubation, cells were collected, washed twice with ice-cold buffer D [30 mM Hepes (pH 7.6), 60 mM KCl, 15 mM NaCl, 50 mM NaF, 10 mM sodium pyrophosphate, 1 mM EDTA, 300 mM sucrose, 1 mM PMSF, 2 μM leupeptin, 2.5 μg/ml aprotinin and 2.5 μg/ml pepstatin A], and then lysed in buffer D containing 0.5% Triton X-100. Labelling of Jurkat cells was essentially the same, except that cells were used at a density of approx. 5×10^6 cells/ml.

For immunoprecipitation of Groucho, cell lysates were mixed with 150 μg/ml of either Groucho monoclonal antibody 3C [18] or preimmune serum and incubated for 2 h at 4 °C in the presence of 1.0 mg/ml BSA. Immunoprecipitates were collected by incubation with Protein G–agarose beads, washed extensively with buffer E [25 mM Tris/HCl (pH 7.8), 200 mM NaCl, 2 mM EDTA, 2 mM EGTA, 50 mM NaF, 10 mM sodium pyrophosphate, 0.5% Triton X-100], and subjected to SDS/PAGE. For immunoprecipitation of TLE1, cell lysates were incubated with either 3 μl of TLE1 serum pre-adsorbed on a glutathione S-transferase (GST)–agarose matrix or 5 μl of preimmune serum. Immunoprecipitates were collected by incubation with Protein A–agarose beads.

Phosphoamino acid analysis was as described in [31]. Phosphoamino acid standards were visualized on dried thin-layer cellulose chromatography plates by ninhydrin treatment, and radioactive phosphoamino acids were localized by autoradiography.

Generation of anti-TLE antibodies

A PCR was used to amplify the DNA regions encoding amino acids 290–387 of TLE1, 214–401 of TLE2 and 350–440 of TLE3. These regions map to the poorly conserved SP domain (domain rich in Ser and Pro residues) of Groucho/TLE proteins [14], and were chosen to provide sequence-specific antigenic determinants. *TLE1* and *TLE3* PCR products were cloned into the pGEM-Tan vector and oligomerized following the protocol described in [32]. Tandemly polymerized *TLE1* (dimer) and *TLE3* (tetramer), as well as monomeric *TLE2*, sequences were then subcloned into pGEX-1N (*TLE1*), pGEX-2T (*TLE2*) or pGEX-3X (*TLE3*) vectors. GST–TLE fusion proteins were induced, isolated and used for immunization of female White New Zealand rabbits as described in [14]. Immune sera were pre-cleared of antibodies against the GST portion of the fusion proteins by affinity chromatography on GST–agarose columns.

Immunoprecipitation and phosphatase treatment of TLE1 proteins from staged P19 cells

Approx. 80 μg of protein from staged P19 cell lysates was incubated in the presence of 3 μl of pre-cleared anti-TLE serum (or 5 μl of preimmune serum) and precipitated with Protein G–agarose beads as described above. Incubation of immunoprecipitated TLE1 proteins and nuclear fractions with calf intestinal alkaline phosphatase was exactly as described in [33].

Pulse–chase studies

Actively growing Jurkat cells were collected by centrifugation, washed with PBS and resuspended in Dulbecco's modified Eagle's medium lacking methionine and cysteine and supplemented with 10% (v/v) fetal bovine serum. After 60 min, the medium received 200 μCi/ml Tran^{35}S label (ICN) and metabolic labelling was performed for 15 min. When no chase with complete medium was performed, cells were collected, washed extensively with ice-

cold PBS and lysed in the presence of buffer F [30 mM Hepes (pH 7.6), 300 mM NaCl, 1 mM EDTA, 20 mM iodoacetamide, 2% Triton X-100, 1 mM PMSF, 2 μM leupeptin, 2.5 μg/ml aprotinin, 2.5 μg/ml antipain, 2.5 μg/ml pepstatin A]. When a chase was performed, cells were washed extensively with PBS and incubated for 60 min in RPMI medium containing 10% (v/v) fetal bovine serum, followed by cell lysis as described above. Lysates were subjected to centrifugation at 12000 ***g*** for 5 min, supernatants were recovered, and immunoprecipitations with anti-TLE1 antibodies or preimmune serum were carried out as described above.

Expression of TLE1 and TLE2 in yeast cells

The *TLE1* and *TLE2* cDNAs were digested with *Eco*RI to generate sequences missing the regions encoding the first 32 and 31 amino acids respectively. *Eco*RI-digested *TLE* cDNAs were subcloned into the *Eco*RI site of the pGBT9 vector in-frame with the DNA-binding domain of the yeast transcription factor GAL4, giving rise to sequences encoding fusions of GAL4 with amino acids 33–770 of TLE1 and amino acids 32–743 of TLE2. Yeast cells were transformed according to the protocol described in [34], and transformed cells were recovered on selective plates lacking tryptophan. Transformed colonies were cultured in YPD (yeast extract/peptone/dextrose) medium, and cells were collected by centrifugation, washed with ice-cold PBS and lysed in electrophoresis sample buffer in the presence of glass beads. The supernatants recovered after centrifugation at 12000 ***g*** for 10 min were subjected to SDS/PAGE and Western blotting with anti-TLE antibodies. The amount of total protein loaded in each lane was estimated after staining the nitrocellulose replicas with Ponceau S.

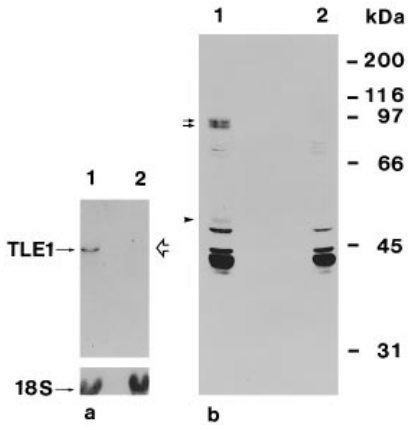

Figure 2 Specificity of anti-TLE1 antibodies in Jurkat and SUP-T1 cells

(**a**) Northern blotting analysis of total RNA (approx. 10 μg/lane) from either Jurkat (lane 1) or SUP-T1 (lane 2) cells with a *TLE1*-specific probe. The 4.5 kb *TLE1* transcript is significantly less abundant in SUP-T1 cells than in Jurkat cells (the open arrow points to the weak hybridization signal observed with RNA from SUP-T1 cells). The result of hybridization with a probe specific for the 18 S rRNA is shown. (**b**) Western blotting analysis of whole-cell lysates (approx. 50 μg of protein/lane) from either Jurkat (lane 1) or SUP-T1 (lane 2) cells with the TLE1 antibodies. Proteins were subjected to SDS/PAGE on a 10% gel, followed by transfer to nitrocellulose. Full-length TLE1 is visualized as a doublet of approx. 90–93 kDa (arrows), which is abundant in Jurkat cells but less so in SUP-T1 cells. An additional immunoreactive species of approx. 50 kDa (arrowhead) is also differentially expressed in the two T lymphoblastic cell lines. The remaining 40–48 kDa bands probably represent cross-reactive species, since their expression levels are identical in Jurkat and SUP-T1 cells. Lanes 1 and 2 are separated by an empty lane to prevent possible spill-over artifacts. Positions of molecular size standards (kDa) are indicated.

RESULTS

Generation of TLE-specific antibodies

We generated polyclonal antibodies against GST–TLE fusion proteins containing regions of TLE1, TLE2 or TLE3 that are poorly conserved among the TLE family (see the Materials and methods section). To demonstrate the specificity of the anti-TLE1 antibodies, we first expressed either a GAL4–TLE1 or a GAL4–TLE2 fusion protein in yeast cells and subjected cell lysates to Western blotting with individual anti-TLE antibodies (Figure 1). The approx. 110 kDa GAL4–TLE1 fusion protein was recognized only by the TLE1 antibodies (lane 1), and not by the TLE2 antibodies (lane 3), the TLE3 antibodies (lane 4) or preimmune serum (lane 2). The TLE1 antibodies did not cross-react with the approx. 105 kDa GAL4–TLE2 fusion protein (lane 6), which was recognized only by the TLE2 antibodies (lane 7) and not by either the TLE3 antibodies (lane 9) or preimmune serum (lane 8). These results thus show that the anti-TLE1 antibodies recognize their target without cross-reacting with TLE2 and that the anti-TLE3 antibodies do not cross-react with either TLE1 or TLE2.

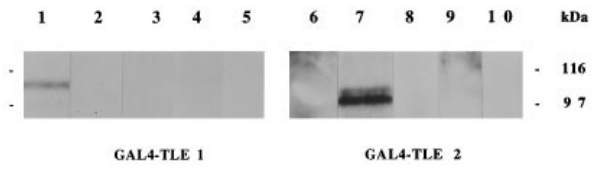

Figure 1 Specificity of anti-TLE antibodies: Western blotting

Whole-cell lysates (approx. 100 μg of protein/lane) from yeast cells expressing either GAL4–TLE1 fusion protein (lanes 1–4) or GAL4–TLE2 fusion protein (lanes 6–9) were subjected to SDS/PAGE on an 8% gel, followed by transfer to nitrocellulose and Western blotting. The GAL4–TLE1 protein is recognized only by the TLE1 antibodies (lane 1) and not by preimmune serum (lane 2), TLE2 antibodies (lane 3) or TLE3 antibodies (lane 4). The GAL4–TLE2 protein, which migrated as a doublet, is recognized only by the TLE2 antibodies (lane 7) and not by TLE1 antibodies (lane 6), preimmune serum (lane 8) or TLE3 antibodies (lane 9). Neither the TLE1 (lane 5) nor the TLE2 (lane 10) antibodies reacted with proteins from control yeast cells that had not been transformed with either the *GAL4–TLE1* or the *GAL4–TLE2* construct. Positions of molecular size standards (kDa) are indicated.

To demonstrate further the specificity of the anti-TLE1 antibodies, we sought to demonstrate a direct correlation between *TLE1* gene expression and TLE1 immunoreactivity. This correlation was provided by the T lymphoblastic leukaemia cell line SUP-T1 [28]. These cells display very low levels of the approx. 4.5 kb *TLE1* transcript (Figure 2a, lane 2) which is expressed at high levels in other cases of acute T lymphoblastic leukaemia cells, such as Jurkat (Figure 2a, lane 1) or CCRF-CEM (results not shown) cells. To determine whether or not the anti-TLE1 antibodies would reveal different immunoreactive profiles in cells expressing different amounts of the *TLE1* message, we performed Western blotting analysis of whole-cell lysates from either Jurkat or SUP-T1 cells. These studies showed that Jurkat cells contain a TLE1 immunoreactive doublet exhibiting an apparent molecular mass in the range 90–93 kDa (Figure 2b, lane 1, see arrows). The mobility of these species corresponds to that expected for full-length TLE1 proteins ([14]; see Figure 5b below). In contrast, we observed only very low levels of this immunoreactive TLE1 component in SUP-T1 cells (Figure 2b, lane 2), consistent with the notion that the 90–93 kDa TLE1 forms are encoded by the *TLE1* message which is transcribed at low levels in SUP-T1 cells. We also observed a faster migrating immunoreactive species of approx. 50 kDa whose expression was

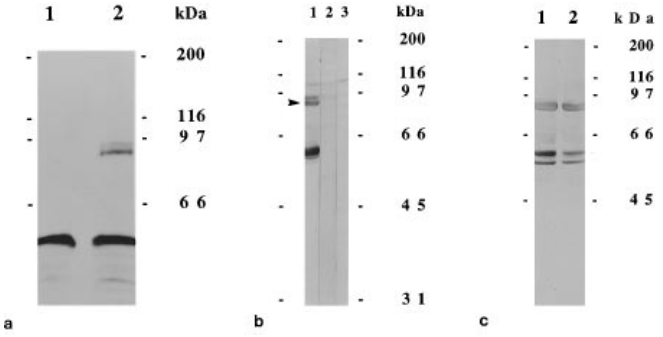

Figure 3 Specificity of anti-TLE3 antibodies

(**a**) Immunoprecipitation with the anti-TLE3 antibodies. Western blotting analysis of proteins immunoprecipitated from HeLa cells with either preimmune serum (lane 1) or the TLE3 antibodies (lane 2). Incubation with panTLE monoclonal antibodies revealed that the TLE3 antibodies immunoprecipitate *bona fide* TLE proteins of approx. 88–90 kDa. (**b**) Western blotting analysis of whole-cell lysates (approx. 80 μg of protein/lane) from HeLa cells with the TLE3 antibodies. Proteins were subjected to SDS/PAGE on a 10% gel, followed by transfer to nitrocellulose. Nitrocellulose replicas were incubated with the TLE3 antibodies alone (lane 1), the TLE3 antibodies in the presence of 10 μg/ml GST–TLE3 fusion protein (lane 2) or preimmune serum (lane 3). The arrowhead points to the position where full-length TLE3 proteins migrate. (**c**) Expression of TLE3 in Jurkat and SUP-T1 cells. Whole-cell lysates (approx. 50 μg of protein/lane) from either Jurkat (lane 1) or SUP-T1 (lane 2) cells were subjected to SDS/PAGE on a 10% gel, followed by transfer to nitrocellulose and Western blotting with the TLE3 antibodies. The expression levels of TLE3 in the two cell lines are identical. Positions of molecular size standards (kDa) are indicated.

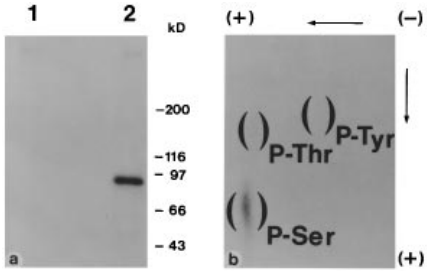

Figure 4 Groucho is a phosphorylated protein

(**a**) Immunoprecipitation of metabolically phosphorylated Groucho. *Drosophila* S2 cells were incubated in the presence of [^{32}P]P_i, followed by cell lysis, immunoprecipitation with either the Groucho monoclonal antibody 3C (lane 2) or preimmune serum (lane 1), and SDS/PAGE. The Groucho antibody precipitated a major phosphorylated protein of approx. 85 kDa. Lanes 1 and 2 are separated by an empty lane to prevent possible spill-over artifacts. Positions of molecular size standards (kDa) are indicated. (**b**) Phosphoamino acid analysis of immunoprecipitated Groucho. Hydrolysis in 5.7 M HCl, first- and second-dimension electrophoresis and visualization of phosphoamino acid standards were as described in the Materials and methods section. The locations of the phosphoamino acid standards visualized on the plate are indicated on the autoradiogram.

reduced in SUP-T1 cells compared with Jurkat cells (Figure 2a, arrowhead). This component probably corresponds to a TLE1 proteolytic product, as indicated by the demonstration that anti-TLE1 antibodies that were affinity-purified using GST–TLE1 fusion proteins immobilized on nitrocellulose reacted with both the 90–93 kDa and 50 kDa proteins (Y. Liu, R. Lo and S. Stifani, unpublished work). These components were not recognized by preimmune serum and were not detected when the TLE1 antibodies were preincubated in the presence of competing amounts of the GST–TLE1 fusion protein, while no competition was observed in the presence of either the GST–TLE2 or the GST–TLE3 fusion proteins (results not shown). Altogether, these results demonstrate that our antibodies are specific for TLE1 and that this protein is mostly present in cultured Jurkat cells as both full-length and faster migrating forms, of approx. 90–93 kDa and 50 kDa respectively. The additional species of lower molecular mass decorated by the anti-TLE1 antibodies correspond to unrelated proteins. This was shown by the observation that they were equally expressed in Jurkat and SUP-T1 cells (Figure 2b, lanes 1 and 2) and were not recognized by affinity-purified anti-TLE1 antibodies (results not shown).

To demonstrate that the anti-TLE3 antibodies recognize true TLE proteins, we subjected HeLa cell lysates to immunoprecipitation with these antibodies and then analysed the immunoprecipitates with monoclonal antibodies that were originally raised against the highly conserved C-terminal end of TLE3 and later shown to be able to recognize the entire TLE protein family (panTLE antibodies [14,19–21]). These studies revealed the presence of *bona fide* TLE proteins in the immunoprecipitate obtained with the anti-TLE3 antibodies (Figure 3a, lane 2). Western blotting analysis visualized TLE3 as both a doublet of approx. 88–90 kDa and a faster immunoreactive species of approx. 60 kDa (Figure 3b, lane 1), a pattern resembling the panTLE immunoreactive profile [14]. These bands were not detected in control experiments with either preimmune serum (Figure 3b, lane 3) or serum that had been preincubated with GST–TLE3 fusion proteins (Figure 3b, lane 2). In contrast, the presence of heterologous GST–TLE fusion proteins had no effect on these interactions, showing that competition was not brought about by the GST moiety (results not shown). TLE3 expression levels were identical in Jurkat and SUP-T1 cells (Figure 3c). The levels of TLE2 and TLE4 were also shown to be identical in these cell lines (J. Yao, Y. Liu, R. Lo and S. Stifani, unpublished work), showing that the *TLE1* gene is differentially expressed in SUP-T1 cells when compared with other *TLE* genes, and that the anti-TLE1 antibodies do not cross-react with other TLE proteins. Altogether, these investigations show that we have obtained specific antibodies that recognize either TLE1 or TLE3.

Groucho/TLE1 proteins are phosphorylated

Groucho/TLE proteins contain a number of conserved phosphorylation sites [14]. To determine whether or not Groucho is phosphorylated, we incubated S2 cells with [^{32}P]P_i, followed by cell lysis and immunoprecipitation with the previously characterized Groucho monoclonal antibody 3C [18]. SDS/PAGE of the immunoprecipitates revealed that Groucho is indeed phosphorylated (Figure 4a, lane 2). Phosphoamino acid analysis revealed that Groucho is mostly phosphorylated on Ser residues (Figure 4b). Phosphorylation was also observed on Thr residues, but only after prolonged autoradiographic exposure or Western blotting with anti-phosphothreonine antibodies (results not shown). No Tyr phosphorylation was detected by either phosphoamino acid analysis (Figure 4b) or Western blotting with anti-phosphotyrosine antibodies (results not shown).

To determine whether TLE1 is also phosphorylated, we subjected Jurkat cells to metabolic labelling with [^{32}P]P_i, followed by cell lysis and immunoprecipitation with the anti-TLE1 antibodies (Figure 5a). These studies demonstrated that TLE1 is a substrate for phosphorylation and migrates as a doublet that is probably composed of two differentially phosphorylated species of approx. 90 and 93 kDa (lane 1, arrows). An approx. 68 kDa phosphorylated protein that was immunoprecipitated by the TLE1 antibodies (arrowhead) was not decorated after Western blotting analysis of the immunoprecipitates with the TLE1 antibodies (results not shown), suggesting that it may correspond

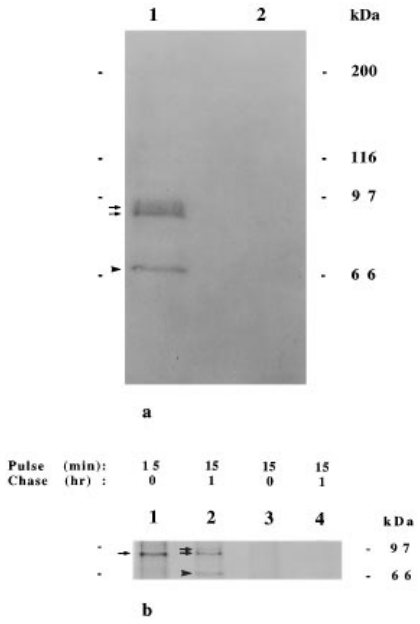

Figure 5 TLE1 is a phosphorylated protein

(**a**) Immunoprecipitation of metabolically phosphorylated TLE1. Jurkat cells were incubated in the presence of [^{32}P]P_i, followed by cell lysis, immunoprecipitation with either the anti-TLE1 antibodies (lane 1) or preimmune serum (lane 2), and SDS/PAGE on an 8% gel. Two phosphorylated proteins of approx. 90 and 93 kDa (arrows) were immunoprecipitated by the TLE1 antibodies. The approx. 68 kDa phosphorylated protein visible in lane 1 (arrowhead) was not decorated by the TLE1 antibodies after Western blotting (not shown). Lanes 1 and 2 are separated by an empty lane. (**b**) Pulse–chase labelling of TLE1 in Jurkat cells. Jurkat cells were cultured, pulse-labelled for 15 min with 200 μCi/ml Tran^{35}S label and harvested either without chase (lanes 1 and 3) or after a 1 h chase (lanes 2 and 4) as described in the Materials and methods section. Cell lysates were immunoprecipitated with either the TLE1 antibodies (lanes 1 and 2) or preimmune serum (lanes 3 and 4), followed by SDS/PAGE. The arrows point to the positions where the 89 kDa TLE1 precursor (lane 1) and the 90–93 kDa TLE1 doublet (lane 2) migrate. The arrowhead points to an approx. 68 kDa species that is immunoprecipitated only after the 1 h chase and is not recognized by the TLE1 antibodies after Western blotting. The gel was loaded leaving empty lanes between samples. Positions of molecular size standards (kDa) are indicated.

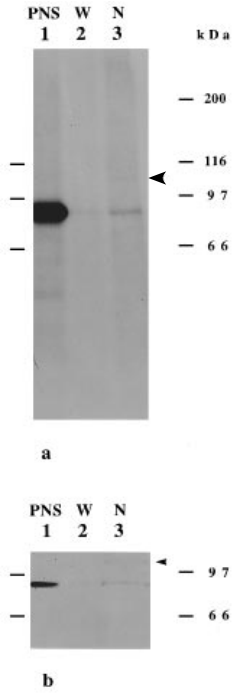

Figure 6 Distribution of Groucho proteins in subcellular fractions

(**a**) Immunoprecipitation of phosphorylated Groucho proteins. S2 cells were grown, metabolically labelled with [^{32}P]P_i and subjected to cell fractionation as described in the Materials and methods section. The total post-nuclear supernatant (PNS; lane 1), the total first nuclear wash (W; lane 2) and the total nuclear fraction (N; lane 3) were subjected to immunoprecipitation with Groucho monoclonal antibodies, followed by SDS/PAGE and autoradiography. An approx. 85 kDa Groucho component was found predominantly in the post-nuclear supernatant (lane 1), while a more slowly migrating component of approx. 110 kDa (arrowhead) was enriched in the nuclear fraction (lane 3). A small amount of the 85 kDa component was also visible in the nuclear wash fraction (lane 2). (**b**) Western blotting analysis with Groucho monoclonal antibodies of the post-nuclear supernatant (PNS; lane 1; approx. 40 μg of protein/lane, corresponding to approx. 30% of the total post-nuclear supernatant), the first nuclear wash (W; lane 2; approx. 30 μg of protein/lane, corresponding to the entire wash fraction) and the nuclear fraction (N; lane 3; approx. 40 μg of protein/lane, corresponding to approx. 75% of the nuclear fraction) from S2 cells. Groucho is detected as a major species of approx. 84–85 kDa in the post-nuclear supernatant (a small amount is visible in the nuclear wash; lanes 1 and 2), while two forms of approx. 85 and 110 kDa (arrowhead) are observed in the nuclear fraction (lane 3). Positions of molecular size standards (kDa) are indicated.

to a co-immunoprecipitated component. We next investigated the biosynthesis of TLE1 by performing pulse–chase studies. Jurkat cells were metabolically labelled with [^{35}S]methionine for 15 min, followed by a 60 min chase, lysis and immunoprecipitation with the TLE1 antibodies (Figure 5b). These studies showed that TLE1 is initially synthesized as an approx. 89 kDa precursor exhibiting the predicted size of full-length TLE1 (lane 1, arrow). After a 60 min chase, however, two immunoprecipitated proteins were observed that exhibited apparent molecular masses of approx. 90 kDa and 93 kDa (lane 2, arrows). These investigations demonstrate that TLE1 is initially synthesized as an approx. 89 kDa precursor; differential phosphorylation of this protein then gives rise to the 90–93 kDa TLE1 doublet. Altogether, our studies show that Groucho/TLE1 proteins are phosphorylated and that phosphorylation reduces their electrophoretic mobility.

Subcellular distribution of Groucho proteins exhibiting different electrophoretic mobilities

We next investigated the intracellular distribution of Groucho by subjecting S2 cells to a previously described cell fractionation procedure [30,35]. Cells were metabolically labelled with [^{32}P]P_i, lysed in a hypotonic buffer and fractionated by low-speed centrifugation into a low-salt-soluble supernatant (post-nuclear supernatant) and a nuclear pellet. The total protein content of each subcellular fraction was then subjected to immunoprecipitation with the Groucho monoclonal antibodies, followed by SDS/PAGE and autoradiography (Figure 6a). These investigations revealed a second phosphorylated Groucho component of approx. 110 kDa (lane 3, arrowhead) in addition to the previously described phosphorylated Groucho species of approx. 85 kDa (lane 1). These two components displayed different subcellular distributions: the faster migrating form was predominantly, but not exclusively, detected in the post-nuclear supernatant, while the 110 kDa component was enriched in the nuclear fraction. We observed the same results when identical amounts of proteins from the post-nuclear supernatant and the nuclear fraction were analysed by Western blotting with Groucho monoclonal antibodies (Figure 6b). A faster migrating form(s) of approx. 84–85 kDa was present predominantly in the post-nuclear supernatant (lane 1), but was also detected in the nuclear fraction (lane 3). In contrast, a more slowly migrating component of approx. 110 kDa (which was only detected weakly) was found

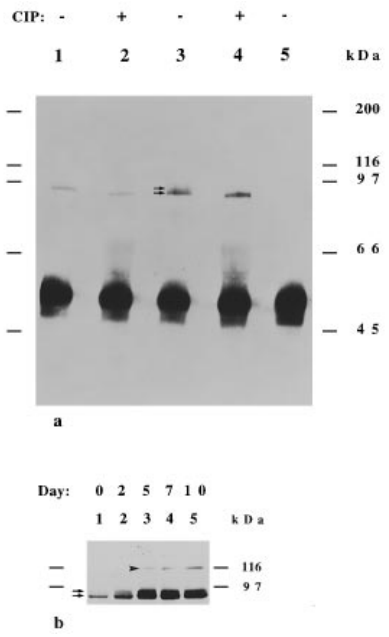

Figure 7 Temporal profile of TLE1 expression in differentiating P19 cells

(**a**) Immunoprecipitation and phosphatase treatment of TLE1. P19 cells were grown and neural induction was performed as described in the Materials and methods section. Whole-cell lysates (approx. 100 μg of protein) from either day 0 (lanes 1 and 2) or day 10 (lanes 3–5) P19 cells were subjected to immunoprecipitation with either the anti-TLE1 antibodies (lanes 1–4) or preimmune serum (lane 5). Following immunoprecipitation, samples were incubated at 37 °C for 30 min either in the presence of 0.4 unit/ml calf intestinal phosphatase (CIP; lanes 2 and 4) or without added phosphatase (lanes 1, 3 and 5). After these incubations, samples were subjected to SDS/PAGE on a 10% gel, followed by transfer to nitrocellulose and Western blotting with TLE1 antibodies. The arrows point to the position of migration of the 90–93 kDa TLE1 doublet. (**b**) Western blotting analysis of staged P19 cell lysates with the TLE1 antibodies. Whole-cell lysates were collected after the indicated number of days, protein contents were standardized by Lowry assay and identical amounts of protein from each time point were subjected to SDS/PAGE on a 10% gel (approx. 80 μg of protein/lane). Following transfer to nitrocellulose, replicas were stained with Ponceau S to verify that the lanes contained equal amounts of protein and then subjected to Western blotting with the TLE1 antibodies. The arrows point to the position of migration of the immunoreactive 90–93 kDa TLE1 doublet. The arrowhead points to the position of migration of the approx. 118 kDa TLE1 form that is induced as a function of differentiation. The faint bands of approx. 130 kDa were also observed with preimmune serum. Positions of molecular size standards (kDa) are indicated.

associated with the nuclei (lane 3, see arrowhead). The observed nuclear interactions were detected even after two sequential washes of the nuclear pellet in hypotonic buffer, indicating that they are not affected by low ionic strength conditions. Altogether, these results show that phosphorylated Groucho proteins exhibiting different apparent molecular masses display different affinities for the nuclear compartment.

TLE1 undergoes changes in its expression profile and phosphorylation during neural differentiation of P19 embryonic carcinoma cells

To further investigate the significance of the previous observations with *Drosophila* S2 cells, we analysed the properties of TLE1 in a dynamic cellular environment that would allow us to monitor TLE1 expression and/or phosphorylation during cell differentiation. We chose to examine the properties of TLE1 in differentiating mouse P19 embryonic carcinoma cells. These pluripotent proliferating cells can be induced to enter the neural lineage by treatment with retinoic acid, leading to the generation of both neuronal and glial cells [29]. We prepared cell lysates from either undifferentiated cells (day 0) or cells that had differentiated for 10 days after addition of retinoic acid (day 10), and subjected identical amounts of protein to immunoprecipitation with the anti-TLE1 antibodies, followed by SDS/PAGE and Western blotting with the antibodies (Figure 7a). These experiments showed that a 90–93 kDa doublet was immunoprecipitated from day 10 lysates (lane 3), while a single 90 kDa component of lower abundance was immunoprecipitated from day 0 lysates (lane 1), showing that there is an increase in the overall amount of TLE1 during neural induction and suggesting that TLE1 becomes increasingly phosphorylated. No other TLE1 immunoreactive proteins could be identified after Western blotting analysis of the immunoprecipitates. To further investigate the temporal profile of TLE1 expression during neural induction, we subjected identical amounts of proteins from staged P19 cells to Western blotting analysis with the anti-TLE1 antibodies (Figure 7b). Before addition of retinoic acid, the TLE1 antibodies detected predominantly a single band with an apparent molecular mass of approx. 90 kDa (lane 1). As neural induction proceeded, the amount of the immunoreactive 90 kDa band increased and a more slowly migrating form with an apparent molecular mass of 93 kDa became gradually more prominent, reaching a peak 5 days after induction (lanes 2–5, arrows). A faster migrating component of approx. 50 kDa resembling the smaller TLE1 species observed in Jurkat cells was also detected; its level gradually increased in parallel with the 90–93 kDa doublet (results not shown). Thus the results of immunoprecipitation and quantitative Western blotting studies are in agreement with each other and indicate that TLE1 becomes more abundant as a function of P19 cell differentiation. We noticed that Western blotting analysis revealed higher amounts of the 93 kDa form when cellular extracts, rather than immunoprecipitates, were analysed (cf. Figure 7a, lane 3, and Figure 7b, lane 5). This observation suggests that the TLE1 antibodies may immunoprecipitate less effectively the more slowly migrating TLE1 species.

We next tested the hypothesis that the 93 kDa form of TLE1 that becomes more abundant during P19 cell differentiation is the product of increased phosphorylation. We subjected immunoprecipitates from either undifferentiated or differentiated P19 cells to incubation with calf intestinal phosphatase, followed by Western blotting with the anti-TLE1 antibodies. These experiments showed that, after phosphatase treatment, the 90–93 kDa components from day 10 lysates were no longer detected; instead, a single species was observed that migrated faster than either form of the doublet (Figure 7a, lane 4). The TLE1 form immunoprecipitated from day 0 lysates was also sensitive to phosphatase treatment and shifted to a lower position (Figure 7a, lane 2). These results thus show that TLE1 is phosphorylated in undifferentiated P19 cells and becomes gradually more phosphorylated during retinoic acid-induced *in vitro* neurogenesis, suggesting that the phosphorylation state of TLE1 is a function of cell differentiation.

Slowly migrating TLE1 proteins are induced during P19 cell differentiation and are tightly associated with the nuclear compartment

Our analysis of the temporal expression pattern of TLE1 also revealed that an approx. 118 kDa immunoreactive band was induced during neural differentiation of P19 cells (Figure 7b, arrowhead). To ascertain whether or not this more slowly migrating species was a true TLE1 protein resembling the 110 kDa Groucho form, we analysed its properties further. First, we subjected adjacent lanes containing fractionated whole-cell

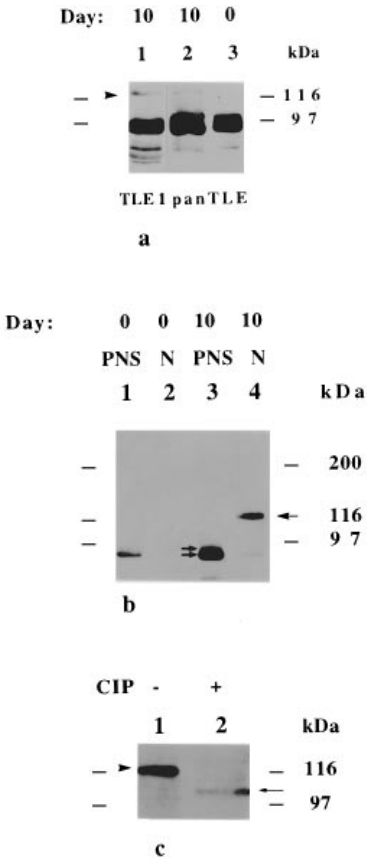

Figure 8 Analysis of the properties of the 118 kDa TLE1 component

(**a**) Detection of the inducible 118 kDa TLE1 form (arrowhead) with panTLE monoclonal antibodies. Whole-cell lysates (approx. 80 μg of protein/lane) from either day 10 (lanes 1 and 2) or day 0 (lane 3) P19 cells were subjected to SDS/PAGE on a 10% gel, followed by transfer to nitrocellulose and Western blotting with either TLE1 (lane 1) or panTLE (lanes 2 and 3) antibodies. (**b**) Subcellular distribution of TLE1 in P19 cells. P19 cells collected either before (day 0; lanes 1 and 2) or 10 days after (day 10; lanes 3 and 4) addition of retinoic acid were subjected to subcellular fractionation, and both the post-nuclear supernatant (PNS; lanes 1 and 3; approx. 50 μg of protein/lane, corresponding to approx. 20% of the total fraction) and the nuclear fraction (N; lanes 2 and 4; approx. 40 μg of protein/lane, corresponding to approx. 60% of the total fraction) were subjected to SDS/PAGE on a 10% gel, followed by transfer to nitrocellulose and Western blotting with the TLE1 antibodies. The arrows point to the position of migration of the 90–93 kDa TLE1 doublet. The arrowhead points to the position of migration of the induced 118 kDa TLE1 form that is enriched in the nuclear fraction from day 10 cells. (**c**) Incubation of day 10 P19 nuclear fractions with alkaline phosphatase. Approx. 50 μg of protein from the nuclear fraction from P19 cells collected 10 days after exposure to retinoic acid was incubated at 37 °C for 30 min either in the presence of 1.2 units/ml calf intestinal phosphatase (CIP; lane 2) or without added phosphatase (lane 1). After this incubation, samples were analysed by Western blotting with the TLE1 antibodies. Phosphatase treatment caused the 118 kDa TLE1 form (arrowhead) to shift to an apparent molecular mass of approx. 108 kDa (arrow). Positions of molecular size standards (kDa) are indicated.

lysates from staged P19 cells to Western blotting with the highly specific panTLE monoclonal antibodies and the TLE1 antibodies (Figure 8a). These investigations showed that the panTLE antibodies also decorated an approx. 118 kDa protein that was absent from undifferentiated cells (lane 3) and present in cells that had been induced with retinoic acid (lane 2). This panTLE immunoreactive species co-migrated with the 118 kDa protein decorated by the TLE1 antibodies (cf. lanes 1 and 2, arrowhead), suggesting that both polyclonal antibodies against TLE1 and monoclonal antibodies against the TLE family recognize the same protein.

We next subjected staged P19 cells to subcellular fractionation to compare the distributions of the TLE1 proteins exhibiting distinct electrophoretic mobilities. Subcellular fractions from either uninduced or induced (day 10) P19 cells were analysed by Western blotting with the TLE1 antibodies. We chose to analyse total fractions rather than immunoprecipitates because our TLE1 antibodies do not effectively immunoprecipitate the 118 kDa TLE1 form (Figure 7a). At both day 0 and day 10, the 90–93 kDa TLE1 doublet was found predominantly in the post-nuclear supernatant (Figure 8b, lanes 1–4). In contrast, the slowly migrating, inducible, TLE1 form of 118 kDa present in day 10 cells was found to be associated with the nuclear fraction (lane 4). These results suggest that different TLE1 species exhibit different affinities for the nuclear compartment: while the more slowly migrating form of 118 kDa is bound to the nuclei after subcellular fractionation, the 90–93 kDa forms either are not associated with the nuclear compartment or can be released from the nuclei by exposure to low ionic strength conditions. [The small fraction of the 90–93 kDa TLE1 doublet that was associated with the nuclear compartment after subcellular fractionation suggests that these proteins can interact with the nuclei (Figure 8b, lane 4).] These results show that TLE1 proteins with different apparent molecular masses display properties analogous to those of the slower and faster migrating Groucho proteins described above. To further test this possibility, we next sought to determine whether or not the 118 kDa protein was phosphorylated. We subjected total nuclear extracts from day 10 P19 cells to incubation with alkaline phosphatase, followed by Western blotting with the anti-TLE1 antibodies (Figure 8c). These studies showed that the 118 kDa species is indeed phosphorylated, since incubation with intestinal phosphatase greatly increased its electrophoretic mobility to an apparent molecular mass of approx. 108 kDa (cf. lanes 1 and 2). These combined results thus show that the 118 kDa TLE1 protein is phosphorylated and displays a strong association with the nuclear compartment, in perfect agreement with the properties of the 110 kDa Groucho proteins. However, these studies did not determine whether the 108 kDa molecule is a product of alternative splicing, a combination of post- and/or co-translational modifications, or other mechanisms.

Altogether, the consistent results observed with different Groucho/TLE proteins, different cell lines and different antibodies show that more slowly migrating forms of TLE1 and Groucho are phosphorylated and display a strong association with the nuclear compartment. In turn, these observations suggest that these higher-molecular-mass molecules may perform nuclear functions important for the activity of Groucho/TLE1 proteins. Finally, our results show that the nuclear 118 kDa TLE1 component is induced as a function of cell commitment in P19 cells, suggesting that this protein may play a role during differentiation.

TLE3 exhibits no apparent changes during neural differentiation of P19 cells

We detected no apparent changes when we monitored the expression profile of TLE3 during neural induction of P19 cells (Figure 9), suggesting that neither the level nor the phosphorylation state of TLE3 changes in response to P19 cell differentiation. Although it is possible that changes in TLE3 phosphorylation were not detected by the anti-TLE3 antibodies, it appears that individual TLE proteins exhibit distinct responses to retinoic acid-induced neural determination of P19 cells, suggesting that different TLE proteins may have distinct properties.

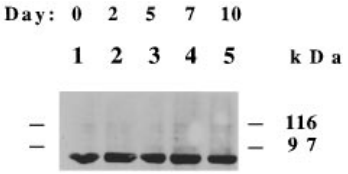

Figure 9 Temporal profile of TLE3 expression in differentiating P19 cells

P19 cells were grown and neural induction was performed as described in the Materials and methods section. Whole-cell lysates were collected after the indicated numbers of days, protein contents were standardized by Lowry assay and equal amounts of protein from each time point were subjected to SDS/PAGE on a 10% gel (approx. 80 μg of protein/lane). Following transfer to nitrocellulose, replicas were stained with Ponceau S to verify that the lanes contained equal amounts of protein and subjected to Western blotting with the TLE3 antibodies. The expression profile of TLE3 did not change during neural induction of P19 cells. Positions of molecular size standards (kDa) are indicated.

DISCUSSION

Characterization of antibodies specific for individual TLE proteins

We are interested in understanding the mechanisms controlling the function of Groucho/TLE proteins and how these events may be regulated in response to changing physiological conditions. To monitor the properties of individual TLE proteins, we have characterized new antibodies that specifically recognize either TLE1 or TLE3. The specificity of the anti-TLE1 and -TLE3 antibodies was demonstrated in a number of ways. First, the former reagents recognize a GAL4–TLE1 fusion protein expressed in yeast, but not a GAL4–TLE2 fusion protein, while the latter antibodies do not recognize either fusion protein even though they can immunoprecipitate *bona fide* TLE proteins (Figures 1 and 3). Secondly, both the TLE1 and the TLE3 antibodies react against bands displaying the sizes expected for full-length TLE proteins [14] (Figures 2, 3, 7 and 9). Their immunoreactive profiles are distinct from each other and from the pattern recognized by the anti-TLE2 antibodies (Y. Liu, R. Lo and S. Stifani, unpublished work). Thirdly, the TLE1 antibodies reveal the presence of a 90–93 kDa TLE1 doublet in lysates from Jurkat acute T lymphoblastic leukaemia cells and show that this component is decreased in protein extracts prepared from the T lymphoblastic leukaemia cells SUP-T1, which exhibit significantly lower levels of *TLE1* gene expression (Figure 2). In contrast, the levels of TLE3 (Figure 3), TLE2 and TLE4 (J. Yao, Y. Liu, R. Lo and S. Stifani, unpublished work) are identical in different types of T lymphoblastic leukaemia cells. These observations provide strong evidence that the TLE1 antibodies recognize the product(s) of the 4.5 kb *TLE1* transcript whose expression is reduced in SUP-T1 cells when compared with other T lymphoblastic leukaemia cells.

It is worth commenting on the possible significance of the decreased TLE1 expression in SUP-T1 cells. This cell line contains a chromosomal translocation that breaks the *Notch1* gene and separates the sequence encoding the extracellular domain of the receptor from the sequence coding for the transmembrane and intracellular domains [28,36]. It is believed that the ensuing neoplastic transformation is the result of 'activating' Notch signalling by deregulating the expression of the Notch1 intracellular domain [37–41]. Since Notch activity was shown to control the expression of other members of the Notch signalling pathway [42–44], it is possible that *TLE1* expression and function may be regulated by oncogenic Notch1 activity in SUP-T1 cells. It is entirely possible, however, that the reduced levels of TLE1 expression in these cells may be an indirect result of the oncogenic transformation.

Groucho/TLE proteins are phosphorylated, and TLE1 phosphorylation correlates with cell differentiation

By using a combination of metabolic labelling, phosphoamino acid analysis and phosphatase digestion, we have demonstrated that Groucho/TLE proteins are phosphorylated (Figures 4, 5 and 7). Furthermore, we have shown that the phosphorylation state of TLE1 is a function of cell differentiation in mouse P19 embryonic carcinoma cells that have been induced to enter the neural lineage by retinoic acid. TLE1, which is present in undifferentiated cells mostly as a 90 kDa phosphorylated species, undergoes an increase in both its cellular level and phosphorylation during cell differentiation, resulting in a gradual increase in the amount of a slightly slower form of molecular mass 93 kDa (Figure 7). These observations are consistent with previous findings with panTLE antibodies showing that more slowly migrating TLE forms of approx. 93 kDa are more abundant in extracts from embryonic neural tissues undergoing active neurogenesis than in those from cultured neural stem cells [20]. Moreover, we have observed a similar increase in the amount of the phosphorylated 93 kDa TLE1 component during the *in vitro* differentiation of CFK2 chondrocytic precursor cells (J. Yao, Y. Liu, R. Lo and S. Stifani, unpublished work). These combined observations suggest that the ratio between the 90 and 93 kDa TLE1 forms changes as a function of differentiation: the former component represents the predominant TLE1 species in undifferentiated cells, while the 93 kDa species becomes more abundant in cells that are undergoing differentiation. These results implicate phosphorylation in the activity of TLE1 during cell commitment. In contrast, we failed to detect changes in TLE3 expression and phosphorylation during P19 neural induction (Figure 9). Together with expression studies showing that individual TLE proteins display similar but non-overlapping patterns ([20]; Y. Liu, R. Lo and S. Stifani, unpublished work), these findings suggest that different TLE proteins may perform non-redundant functions.

More slowly migrating forms of Groucho and TLE1 display increased affinity for the nuclear compartment

Our analysis of TLE1 expression also shows that a more slowly migrating form of TLE1 with an apparent molecular mass of approx. 118 kDa becomes more abundant during P19 cell differentiation. This protein is recognized by both TLE1 and panTLE antibodies (Figures 7 and 8) and resembles a higher-molecular-mass form of Groucho of approx. 110 kDa which is observed in *Drosophila* S2 cells (Figure 6) and embryos (results not shown). These findings, together with the identification of more slowly migrating forms of TLE2 of approx. 110 kDa (Y. Liu, R. Lo and S. Stifani, unpublished work), indicate that Groucho/TLE protein populations are heterogeneous in size. Moreover, the observation that the 118 kDa species is induced as a function of P19 cell differentiation suggests that this TLE1 form may perform an important role during cell determination. Our studies establish a functional correlation between the 110 kDa Groucho protein and the 118 kDa TLE1 component. Both of them are tightly associated with the nuclear compartment after subcellular fractionation of insect and mammalian cells respectively (Figures 6 and 8). In contrast, the faster migrating Groucho and TLE1 species of 84–85 and 90–93 kDa respectively

are predominantly recovered in the post-nuclear supernatant. Previous immunohistological analysis of both *Drosophila* embryos [18] and mammalian tissues [14,19–21] has revealed that Groucho/TLE immunoreactivity is mostly localized to the nuclear compartment in intact cells. However, this nuclear immunocytochemical reactivity is either lost or greatly reduced when cells grown on coverslips are exposed to low ionic strength conditions prior to fixing with paraformaldehyde ('*in situ* lysis'; [35]) (R. Lo and S. Stifani, unpublished work). Altogether, these results suggest that Groucho/TLE1 proteins with different apparent molecular masses are associated with the nuclear compartment in intact cells, but the strength of their nuclear interaction is different. Higher-molecular-mass forms are more tightly bound than smaller forms, although both can translocate to the nuclei. More slowly migrating forms may be capable of participating in molecular interactions important for their nuclear tethering, while smaller forms may lack this ability and thus can be eluted from the nuclear compartment during subcellular fractionation.

Although the molecular mechanisms underlying the different affinities for the nuclei of the smaller and larger Groucho/TLE1 components are unknown, our studies suggest that phosphorylation reactions may play a role in these events. The phosphorylation state of the larger proteins may be different from that of the faster migrating forms, and this difference may play a role in the nuclear association of these proteins. However, although we have shown that removal of phosphate groups by incubation with calf intestinal phosphatase, a broad-spectrum enzyme, significantly increases the electrophoretic mobility of the 118 kDa TLE1 component (Figure 8), phosphorylation alone cannot account for the fact that the 118 kDa TLE1 species migrates significantly more slowly than the 90–93 kDa doublet. Dephosphorylation of the former only changes its apparent molecular mass to approx. 108 kDa and not to approx. 89 kDa, the size expected for unphosphorylated TLE1 (Figures 5 and 7). Although dephosphorylation of the 118 kDa protein may not be completely achieved using calf intestinal phosphatase, our results suggest that in P19 cells the 118 kDa TLE1 species may represent a phosphorylated form of a product of alternative splicing, other post- and/or co-translational modifications, or other mechanisms. The availabilty of the anti-TLE1 antibodies and of an inducible experimental system such as the P19 cells will facilitate future studies aimed at understanding the role of the higher-molecular-mass TLE1 proteins.

We thank S. Artavanis-Tsakonas, in whose laboratory some of these studies were initiated, Lakshmi Bangalore for invaluable help during phosphoamino acid analysis, Ruth Slack and Freda Miller for assistance with the P19 cells, Josh Socolow and Yoav Timsit for help during the generation of the TLE antibodies, and Yanling Liu for excellent technical assistance. This work was supported by grants to S.S. from the Medical Research Council of Canada (MRC PG11473) and the Human Frontier Science Program (RG-490/94). S.S. is a Scholar of the Fonds de la Recherche en Sante du Quebec.

REFERENCES

1 Ghysen, A., Dambly-Chaudiere, C., Jan, L. Y. and Jan, Y.-N. (1993) Genes Dev. **7**, 723–733
2 Artavanis-Tsakonas, S., Matsuno, K. and Fortini, M. E. (1995) Science **268**, 225–232
3 Rebay, I., Fleming, R. J., Fehon, R. G., Cherbas, L., Cherbas, P. and Artavanis-Tsakonas, S. (1991) Cell **67**, 687–699
4 Diederich, R. J., Matsuno, K., Hing, H. and Artavanis-Tsakonas, S. (1994) Development **120**, 473–481
5 Fortini, M. E. and Artavanis-Tsakonas, S. (1994) Cell **79**, 273–282
6 Hartley, D. A., Preiss, A. and Artavanis-Tsakonas, S. (1988) Cell **55**, 785–795
7 Preiss, A., Hartley, D. A. and Artavanis-Tsakonas, S. (1988) EMBO J. **7**, 3917–3927
8 Rushlow, C. A., Hogan, A., Pinchin, S. M., Howe, K. R., Lardelli, M. T. and Ish-Horowicz, D. (1989) EMBO J. **8**, 3095–3103
9 Orenic, T. V., Held, L. I., Paddock, S. W. and Carrol, S. B. (1993) Development **118**, 9–20
10 Delidakis, C. and Artavanis-Tsakonas, S. (1992) Proc. Natl. Acad. Sci. U.S.A. **89**, 8731–8735
11 Knust, E., Schrons, H., Grawe, F. and Campos-Ortega, J. A. (1992) Genetics **132**, 505–518
12 Williams, F. E. and Trumbly, R. J. (1990) Mol. Cell. Biol. **10**, 6500–6511
13 Keleher, C. A., Redd, M. J., Schultz, J., Carlson, M. and Johnson, A. D. (1992) Cell **68**, 708–719
14 Stifani, S., Blaumueller, C. M., Redhead, N. J., Hill, R. E. and Artavanis-Tsakonas, S. (1992) Nature Genet. **2**, 119–127
15 Mallo, M., Franco del Amo, F. and Gridley, T. (1993) Mech. Dev. **42**, 67–76
16 Miyasaka, H., Choudhury, B. K., Hou, E. W. and Li, S. S.-L. (1993) Eur. J. Biochem. **216**, 343–352
17 Schmidt, C. J. and Sladek, T. E. (1993) J. Biol. Chem. **268**, 25681–25686
18 Delidakis, C., Preiss, A., Hartley, D. A. and Artavanis-Tsakonas, S. (1991) Genetics **129**, 803–823
19 Zagouras, P., Stifani, S., Blaumueller, C. M., Carcangiu, M. L. and Artavanis-Tsakonas, S. (1995) Proc. Natl. Acad. Sci. U.S.A. **92**, 6414–6418
20 Dehni, G., Liu, Y., Husain, J. and Stifani, S. (1995) Mech. Dev. **53**, 369–381
21 Liu, Y., Dehni, G., Purcell, K. J., Socolow, J., Carcangiu, M. L., Artavanis-Tsakonas, S. and Stifani, S. (1996) Genomics **31**, 58–64
22 Paroush, Z., Finley, R. L., Kidd, T., Wainwright, S. M., Ingham, P. W., Brent, R. and Ish-Horowicz, D. (1994) Cell **79**, 805–815
23 Ohsako, S., Hyer, J., Panganiban, G., Oliver, I. and Caudy, M. (1994) Genes Dev. **8**, 2743–2755
24 Van Doren, M., Bailey, A. M., Esnayra, J., Ede, K. and Posakony, J. W. (1994) Genes Dev. **8**, 2729–2742
25 Fehon, R. G., Kooh, P. J., Rebay, I., Regan, C. L., Xu, T., Muskavitch, M. A. and Artavanis-Tsakonas, S. (1990) Cell **61**, 523–534
26 Schwenk, H. U. and Schneider, U. (1975) Blood **31**, 299–306
27 Foley, G. E., Lazarus, H., Farber, S., Uzman, B. G., Boone, B. A. and McCarthy, R. E. (1965) Cancer **18**, 522–529
28 Ellisen, L. W., Bird, J., West, D. C., Soreng, A. L., Reynolds, T. C., Smith, S. D. and Sklar, J. (1991) Cell **66**, 649–661
29 Rudnicki, M. A. and McBurney, M. W. (1987) in Teratocarcinomas and Embryonic Stem Cells: A Practical Approach (Robertson, E. J., ed.), pp. 19–49, IRL Press, Oxford
30 Dignam, J. D., Lebovitz, R. M. and Roeder, R. G. (1983) Nucleic Acids Res. **11**, 1475–1489
31 Apel, E. D., Litchfield, D. W., Clark, R. H., Krebs, E. G. and Storm, D. R. (1991) J. Biol. Chem. **266**, 10544–10551
32 Graham, G. J. and Maio, J. J. (1992) BioTechniques **13**, 780–789
33 Kaffman, A., Herskowitz, I., Tjian, R and O'Shea, E. K. (1994) Science **263**, 1153–1156
34 Schiestl, R. H. and Gietz, R. D. (1989) Curr. Genet. **16**, 339–346
35 Mittnacht, S. and Weinberg, R. A. (1991) Cell **65**, 381–393
36 Aster, J., Pear, W., Hasserjian, R., Erba, H., Davi, F., Luo, B., Scott, M., Baltimore, D. and Sklar, J. (1994) Cold Spring Harbor Symp. Quant. Biol. **59**, 125–136
37 Struhl, G., Fitzgerald, K. and Greenwald, I. (1993) Cell **74**, 331–345
38 Coffman, C. R., Skoglund, P., Harris, W. A. and Kintner, C. R. (1993) Cell **73**, 659–671
39 Fortini, M. E., Rebay, I., Caron, L. A. and Artavanis-Tsakonas, S. (1993) Nature (London) **365**, 555–557
40 Lieber, T., Kidd, S., Alcamo, E., Corbin, V. and Young, M. W. (1993) Genes Dev. **7**, 1949–1965
41 Rebay, I., Fehon, R. G. and Artavanis-Tsakonas, S. (1993) Cell **74**, 319–329
42 Jennings, B., Preiss, A., Delidakis, C. and Bray, S. (1994) Development **120**, 3537–3548
43 Jennings, B., de Celis, J., Delidakis, C., Preiss, A. and Bray, S. (1995) Development **121**, 3745–3752
44 Jarriault, S., Brou, C., Logeat, F., Schroeter, E. H., Kopan, R. and Israel, A. (1995) Nature (London) **377**, 355–358

Received 15 January 1996/11 March 1996; accepted 27 March 1996